



Reserve Estimation of Silica Sand Deposits by Core Control and Geophysical Methods, A Case Study from Saudi Arabia

G. Alsulaimani¹, M.F. Ahmed^{2*} and M.A. Raza³

¹Department of Geological Engineering, Missouri S&T Rolla, MO, USA

²Department of Geological Engineering, University of Engineering and Technology, Lahore, Pakistan

³Department of Mining Engineering, University of Engineering and Technology, Lahore, Pakistan

gsadn9@mst.edu; mfageo@hotmail.com; azeem@uet.edu.pk

ARTICLE INFO

Article history :

Received : 20 June, 2016

Revised : 02 August, 2016

Accepted : 15 August, 2016

Keywords:

Silica sand

GPR

Reserve Estimation

Surface Waves

Core Control

ABSTRACT

This paper summarizes a study carried out for the reserve estimation of silica sand deposits by core control and geophysical data in southern Dawmat Al Jandal, Al Jawf in Saudi Arabia. The study demonstrates the comparison of the data acquired from both core control and geophysical methods. The geophysical techniques applied for this study included the Ground penetrating radar (GPR) and multichannel analysis of surface waves (MASW) to estimate the thickness of surficial silica sand deposits in the study area. The GPR survey acquired 1620 linear meters of ground data across the tape to image internal reflections within the sand deposits up to the contact with underlying sandstone along with 27 MASW field records acquired at different locations by generating 1-D and 2-D shear wave velocity profiles. The results obtained from both of the geophysical investigation techniques were satisfactory and further validated with the core holes data and values.

1. Introduction

The application of Geophysical methods have shown significant growth in recent years after gaining enormous acceptance in fields of geological, geotechnical, and in mining areas [1, 2, 3]. These techniques generally applied to obtain detailed near surface information in terms of layers thickness, economic mineral deposits, depth of bedrock and lithology. Geophysical investigations are an excellent alternative to the conventional core hole methods to provide information of 1-D or 2-D, easy field acquisition, processing and interpenetrations. These tasks can be performed by using the principles of electromagnetic radiation pulses and seismic acoustical wave propagation that are sent out at predetermined distances for data acquisition, processing, and interpretation. These kinds of investigations are generally limited to shallower depths, especially less than 30 meters.

GPR provides detailed information about the subsurface such as the geological structures, folds, strata sequences, utilities, tombs, ancient graves, landmines, and it estimates the thickness of different earth materials, such as soils [4, 5] which are site-dependent. The GPR data is recorded digitally and requires extensive post-acquisition processing, that can be done either in the field or in the office. There are many different GPR processing and analysis techniques [6]. However, the core point data

quality is more reliable in subsurface investigations.

Multichannel Analysis of Surface Waves (MASW) is an advance geophysical method, first introduced to the industry by the Kansas Geological Survey early this century [7, 8]. This method applies the relationship between surface waves and shear waves to ultimately produce a subsurface shear wave velocity profile. The MASW method includes the inversion of a wave that samples an area approximately as wide as it is deep, which provides a smoothed profile of what really exists in the subsurface [9]. It has been commonly applied in mining exploration to determine the depths and thicknesses of the geological strata at a potential mine site. It may also be applied on much smaller scales in the transportation industry to identify damaged areas on asphalt or concrete pavements with high resolution" [10]. The main advantages of the MASW seismic technique is the strength of the utilized surface wave, much greater than the other wave forms; therefore surface waves are more discernible even in the existence of noise. In a record presenting good signal to noise (S/N) ratio, the signal strength of the surface wave should be evident by the linear sloping features of the dispersive wave forms. Surface waves, on an active shot record, are often identified by the smooth sloping behavior as the wave travels down the geophone array [11]. The linear slope represents the phase velocity of the particular surface

* Corresponding author

wave, and can be used to transform the shot record data into a dispersion curve, relating phase velocity to wave frequency [12].

Unconfined Economic Value is one of the primary parameters by which Silica sands are evaluated for their usefulness as manufacturing materials. The unconfined Silica rate of sand is known to be controlled by such factors as depositional environment, transportation routes, bedding orientation, presence of micro fractures, and petrographic characteristics (grain size, grain shape, matrix-cement mineralogy, etc.).

Geophysical survey methods have been used for geological applications (in terms of mapping thick silica sands) to better understand depositional environment. This type of study could be helpful to evaluate the thickness of the sand deposits to get familiar with the depositional environments under favorable conditions. These methods are adequate to detect and delineate local features such as to map loose deposits (i.e. thickness of sand beds), for potential economic interest that could otherwise be very expensive to discover by extensive drilling programs. The application of geophysical surveying could enhance exploration operations by maximizing the ground coverage and minimizing the drilling cost.

This study considered being the first type of investigation using geophysical applications in the region. The geophysical techniques applied for this study included the Ground penetrating radar (GPR) and multichannel analysis of surface waves (MASW) to estimate the thickness of surficial silica sand deposits in the study area. The results were validated with the drilled cores holes observations. Both of these methods showed satisfactory correlation with the core holes measurements made on silica sand deposits in southern Dawmat Al Jandal, Al Jawf in Saudi Arabia.

2. Overview of the Study

In Saudi Paninsula the siliceous material and sandstone most commonly belong to Paleozoic, Mesozoic, and Cenozoic ages that limit the Arabian shield surrounded by the north, east, and south. The silica sand deposits of the upper part of Sirhan Formation are located about 44 km to the south of Dawmat Al Jandal town [13]. The Sirhan Formation is described as a Tertiary unit, mainly composed of white sands, characterized by small hills (with varying thickness of 10 - 40 m) and underlying slightly consolidated sandstone (Fig. 1).

The Sirhan Formation sands and sandstones with having total thickness of 100m are believed to be Miocene and perhaps partly Pliocene in age [13]. Through geological processes of transportation, sedimentation, and erosion lead to purification of the sand and the expulsion of material less stable.

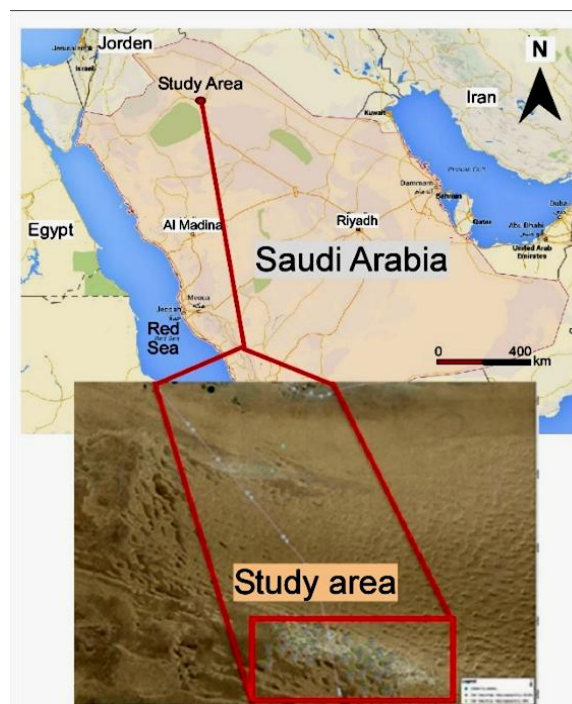


Fig. 1: Location map of the study area

2.1 Estimated Silica Reserves at the Study Area

The sand deposits consist predominantly of well-sorted white silica sands covering an area of about 20 km². The average thickness of sands in the study area was found 20 m. On the basis of drilling results, the average thickness of silica sand as 16m and total estimated reserve is about 160 million tons. The source of silica sands is predominantly quartz with the following average contents: silica 97%, iron oxide 0.2%, and alumina 1.4%. Sands are fine- to coarse-grained and moderately-well sorted. Quartz particles are sub-rounded to sub-angular. The bedding planes observed within the sandstone sequence were apparent and graded horizons that indicate the deposition from multi sedimentary cycles (see outcrop in Fig. 2). The unit displays regular vertical joints and fractures without filling materials.



Fig. 2: White silica sand outcrop of the Sirhan formation (photo by the authors)

3. Methodology

3.1 Ground Penetrating Radar (GPR)

Ground penetrating radar (GPR) contains the transmission of microwave range electromagnetic radiation into the subsurface and the recording of the arrival times and magnitudes of energy that is reflected from features or interfaces in the subsurface [14].

In summary, ground penetrating radar data was acquired at the sites. The lower frequency GPR antenna imaged the subsurface to depths of only 20 meters, so the top of the bedrock in the study areas could not be mapped using this technique.

The radar data were acquired using the SIR-3000 ground penetrating radar instrument which can be used on the ground's surface or in core holes. The antennae with operating frequencies of 100 and 200 MHz were chosen for measurements of the resolution and the penetrating depth thickness of the silica sand deposits (Fig. 3). Studies were conducted at twenty-seven selected sites. A total of 1620 linear meters of ground penetrating radar (GPR) data were collected across the tape that was stretched 30 meters each time. The measurements were taken against the profile distance and each recording (trace) associated with the depth below the surface. The measured microwave radar propagation velocity correlates well to the root of the material constant. With a good estimate of the propagation velocity, images with respect to travel time (two-way travel time down and the time needed to return to the surface) can be transformed directly to respective output images with depth. The GPR data was recorded digitally and processed by using core point analysis techniques [6] by using RADANTM (Radar Data Analyser) software package, prepared by Geophysical Survey Systems Inc. (GSSI).

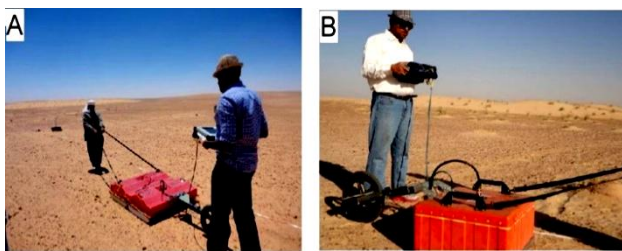


Fig. 3: A) 100 MHz - shielded antenna, and B) 200 MHz - shielded antennae, used in the study area

3.1 Multichannel Analysis of Surface Waves (MASW)

The multichannel Analysis of Surface Waves (MASW) is another powerful method that uses the surface waves for defining subsurface layering, measuring thickness and depth of bedrock. This method is non-invasive, convenient, and least expensive. This method can be utilized to generate both, a single 1-D VS and 2-D VS profiles that cover a wide range of area. This means that the 1-D representations of all twenty-seven sites are

approximately the same, with less variations in subsurface that shows a homogeneous layer of soil which is why the 2-D tomography developed in the study area is capable to represent both depth and distance. The MASW software will provide high resolution on surfaces that are not weathered, that do not possess excessive reflection areas, and that are of uniform thickness and strength [10].

Twenty-seven surface waves and S-wave profile surveys were conducted in the study area. This technique provides a deeper and larger coverage for imaging the subsurface, and for accurately estimating the shear wave velocity of structures more quickly through two-dimensional (1-D, 2-D) tomography of soil layers at depths that are less than or equal to 30 meters [15]. The outline of the MASW method along with a rapid 2-D tomography approach for subsurface investigations is shown in Figure 4. During data acquisition in applying MASW method, a specific number of receivers (N) were linearly arranged with an even spacing (Dx) with distance (XT) and a seismic source was located at a specified distance (X0) away from the first receiver. The identical source-receiver arrangement (SR) was applied by following certain interval (dSR) at various locations to acquire multiple records.

The acquisition of the MASW data is relatively straightforward as shown in Figure 4. There were Twenty-four vertical geophones with 4.5 Hz frequency, placed at 1.0 meter intervals centred on each test location. Acoustic energy was produced at an offset of 8.0 meters (distance to an adjacent geophone), using an accelerated weight of up to (90.71 kg) 200 lb. The Rayleigh wave data were recorded by using a 24-channel signal enhancement seismograph named "Strata view" developed by Geometrics Inc. USA. The acquired Rayleigh wave data were further processed in the Kansas Geologic Survey (KGS) software package "SurfSeis" [15, 16]. This software can process shot records and extract dispersion curves through the initial processing sequences [17]. The seismograph recorded the frequency and the travel time of the seismic waves propagating through the subsurface those were later compared with the frequencies measured at particular depth [10].

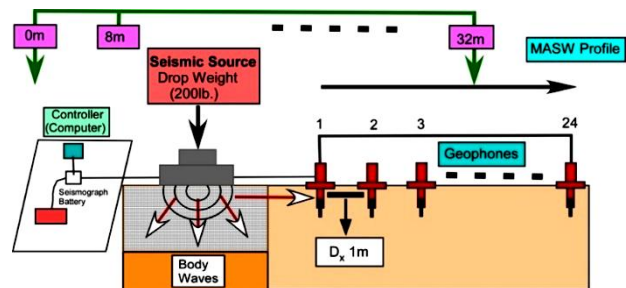


Fig. 4: Schematic MASW field data acquisition layout

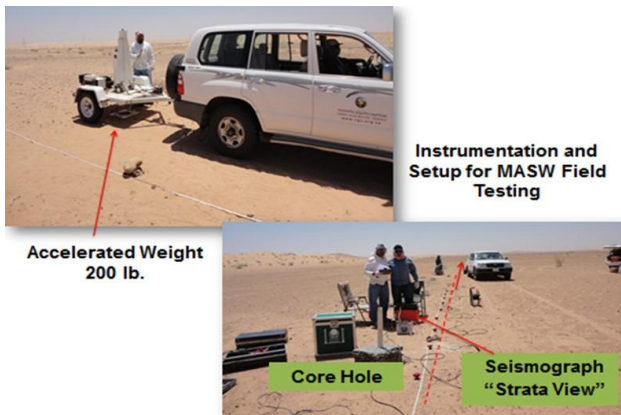


Fig. 5: Field MASW survey layout profiling at Dawmat Al Jandal, Al Jawf

The site-specific dispersion curves, obtained from Rayleigh wave field data and converted into vertical shear wave velocity profiles (see Fig. 6). The inverted 1-D shear wave velocity profiles reached an average depth of 23 meters. Interpolating and contouring of a series of inline 1-D profiles results in a 2-D shear wave velocity profile. By incorporating the existing information into 2-D shear wave velocity profiles from which one could depict the top surface of the bedrock.

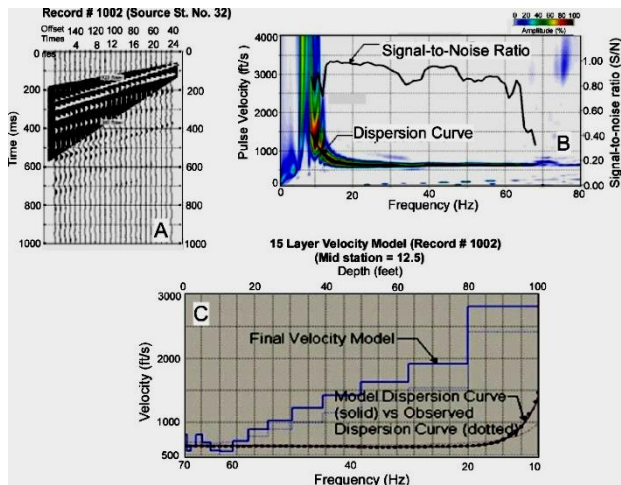


Fig. 6: Dispersion curves, produced for the acquired Rayleigh wave data set. A) Acquisition seismic time series data, B) Surface wave energy in the frequency domain with the observed dispersion curve was transformed (inversion), and C) shear wave velocity vs inversion model depth curve

Processing and analysing of each acquired multichannel surface wave shot, showed a relatively wide frequency bandwidth reflecting an adequate resolution within a few meters below the ground's surface to a depth of more than 30 meters. Dispersion curve analyses were then performed for each shot gathered and derived from the measurements at twenty-seven core holes by exploring the change in phase velocity against frequency

with the help of fundamental mode component of the dispersion data. Non-linear inversion modelling of each dispersion curve resulted in a 1-D mid-point representation of Vs. Interpolation of the 1-D data was done by using a Kriging algorithm which produced a 2-D grid from the input Vs data. Colour-filled contoured profile were also produced from the Vs grid data.

4. Results and Discussions

4.1 GPR

The accurate interpretation of GPR data is dependent on the nature and appropriateness of data processing. The variation in sediment content often relates to both changes in sediment porosity and permeability, which in turn is dependent on changes in grain size and fabric often associated with lamination, cross-bedding, and bounding surfaces. Emmett et al., 1971 [18] observed that porosity and permeability, when parallel to the cross-bed laminate, are higher than when they are perpendicular to the laminate.

There are two major factors that may cause issues when interpreting GPR data: the presence of clay minerals and very inhomogeneous materials. The survey area was found to be very transparent (i.e. clean sands) to GPR signals, and exploration depths in excess of 20 meters were achieved in most of the area. The broad area covered with GPR allowed a clear understanding of the plain sandy area structure.

Two strong reflectors were observed over the area and these were interpreted to be major bounding surfaces.. The first strong reflector results showed a contrast in the electrical impedance between the silica sand and the quartz-rich sand (SiO₂) content of 97 percent, iron oxide 0.2 percent, and alumina 1.4 percent. The chemical analysis of the core holes further confirmed the subsurface deposits of the silica sand

The second major reflector occurred at the boundary between the layers in the sandy plain area, the outcrops mainly consist of white quartz sand white, and greenish and yellowish sandstone layers. The randomly distributed particle size distributions were composed of fine to medium and coarse grained sands within the sandstone sequence with apparent and frequent graded bedding horizons that indicate multi-sedimentary cycles. Also, joints and fractures without filling materials.

The output data displays the velocity analysis of the radargram obtained along with average thicknesses ranging from 8 to 22 meters (Fig. 7). Synthetic hyperbolas with a velocity and the corresponding 2-D ground model for each of the sites were collected along the same survey line over homogeneous silica sand and sand with gravel. The increased shallow resolution for the higher frequencies, offset by the shallower depth of penetration was also evident. The recording time of the two windows

in each survey in this study shows the No of layers and the depth based on expected increase, exhaustive of penetration with decreasing dominant frequency. The measurements recorded from 200MHz frequency source, offered the best vertical resolution for up to 8 meters depth, as there was no coherent signal within the deeper portion of the image. Similarly for the 100MHz source, the information was collected beyond 20-22 meters but with the intermediate resolutions. In short the higher frequencies in the 200 MHz image offer the best vertical resolution with up to 8m depth, and the 100MHz image has intermediate resolution with the greater achieved for this study.

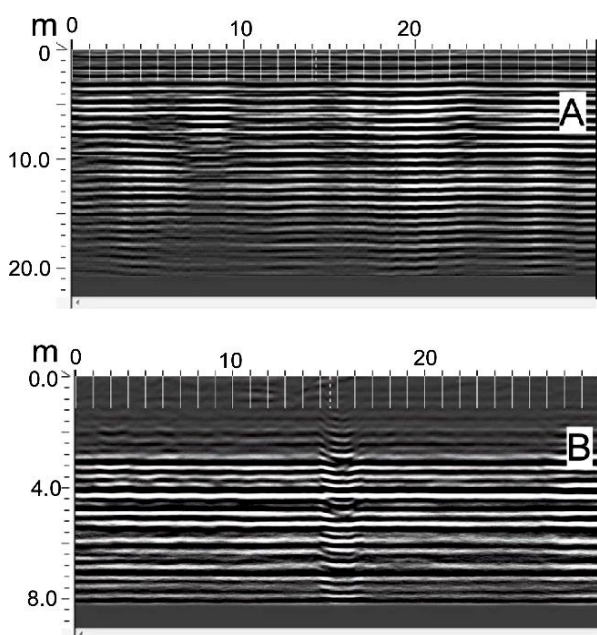


Fig. 7: Radar profile images along the same survey line for an antennae frequency of, A) 100MHz and, B) 200MHz

4.2 MASW

The results of MASW survey include; the S-wave velocities vs depth plots of subsurface layers. 1-D Velocity profiles were derived from the dispersion curve, the travel time distance curves, and the adjacent 2-D ground model for all sites. They are described on the bases of the “ties” between the MASW profiles (1-D & 2-D) and the available core control data (Geo-seismic cross section along profile JSSD-10). Figure 9 shows an example of the depth velocity model of this profile. The interpretation of the shear wave images was carried out to approximate them to be the only layer. The first layer (top layer) identified with velocity (V_s) in the range of 400-610 m/s is a friable fine silica sand cover corresponding to a depth about of 35.0 meters, followed by the top of the bedrock at 1-D, 2-D.

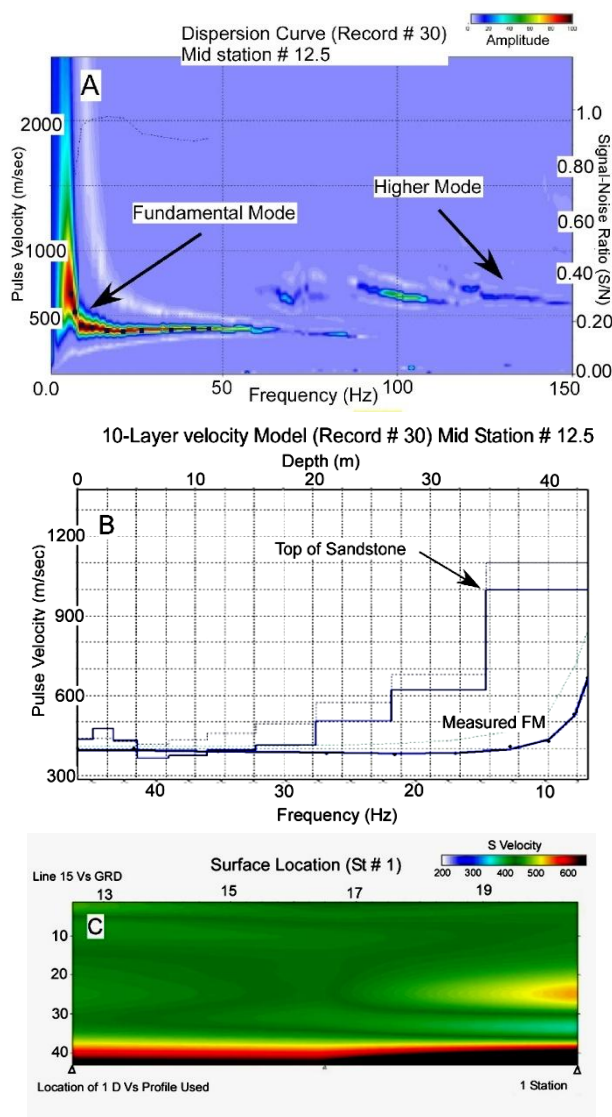


Fig. 8: JSSD-10: (A) Dispersion curve, (B) 1-D shear wave velocity profile, (C) 2-D shear wave velocity model

Although, the Figure 8 (B&C) shows 10-layer velocity models, the interpretation of shear wave images were carried out to approximate them s one or two layers. The first layer (top layer) that identified with velocity (V_s) in the range of 320-450 m/s is friable fine silica sand with an average thickness from 4 - 23.5 meters. White silica sand was identified as the second layer with shear wave velocity (V_s) in the range of 450-700 m/s, covering up to the depth of 16 - 35 meters. In some locations the top of the bedrock was found deeper than 30 meters, and could not be traced. At these locations, the bedrock was presumed to be greater than 30 meters, with a velocity (V_s) much greater than 700 m/s. The strong nature of the surface wave energy may be advantageous when using a simple impact supply, followed by a simple field supply and process. Most significantly the surface waves respond effectively to various types of subsurface deformations

Table 1: Log of the vertical section core hole JSSD 10

Depth (m)		Description	SiO ₂ %
From	To		
0.0	1.50		96.00
1.50	2.90		97.05
2.90	4.50		97.35
4.50	6.00		98.00
6.00	7.50		96.95
7.50	9.00		98.10
9.00	10.50		97.00
10.50	12.00		97.20
12.00	13.00	(From depth 0.0 to 22.70)	96.35
13.00	14.60	Light brownish from	95.1
14.60	15.10	0.0 – 0.60 cm after that off	97.25
15.10	16.50	white silica sand, fine grain, friable	95.00
16.50	18.00		96.10
18.00	18.75		88.35
18.75	19.50		96.00
19.50	20.50		97.05
20.50	21.50		97.35
21.50	22.70		98.00
22.70	24.00	Grayish – silica sand, fine grain, friable	96.95

that are common targets of geological investigations. Continuous recording of multichannel surface waves shows great promise in mapping the top of the bedrock. Cross sections were generated based on data containing information from the horizontal and vertical extension of deposited materials, as shallow as a fraction of a meter down to depths of more than 30 meters, depending on the frequency content.

5. Validation

Twenty-seven core holes with an average depth of 20 m, were drilled in the study area of 20 km² (Fig. 9). These core holes were drilled perpendicular to the geophysical survey lines in order to compare the survey results. In order to cut short the unnecessary drilling expense the investigation was limited to 20-22m in sands. In most cases the depth of bedrock was not reached.

The basic classification of sandstone and silica / quartz material was performed by chemical analysis on the samples obtained from the field. The analysis showed, the silica contents of the cores are greater than 97% (see Table.1). In many industrial applications, the particle size distribution (PSD) of the silica sand is very important. In glass making, the required grain size is

between 0.1 and 0.5 mm, or in some cases, 0.1– 0.63mm, oversized particles prolong the glass batch melting point while the undersized particles cause air bubbles and weaken the glass products. In the study area the grain size diameter was found between 0.1 to 0.5 mm which best suitable size for glass industry. Overall particle shape of sand grains ranges in the category of sub-rounded to sub-angular with small fraction of rounded particles. There were no true bedding features observed within the sand as all of the samples were characterized as friable fine sand.



Fig. 9: Core hole logging of silica sands

Table 2: A comparison of thickness of silica sand deposits by the actual core holes measurement and those obtained from the GPR and MASW methods

Line No.	Coordinate		Core hole (m)	GPR		MASW	Refraction
	Lat N	Long E		Antenna 100 MHz		2-D	2-D
				(m)	(m)	(m)	(m)
JSSD-1	29.45486	39.85944	18	23.5	26.5	22	14
JSSD-2	29.47075	39.87194	21.1	21	19	16	13.5
JSSD-3	29.46544	39.89178	22.7	21	31	30	16
JSSD-4	29.46111	39.91133	17.8	21.5	27.5	28	13
JSSD-5	29.478	39.91631	13.7	21.5	23.5	30	12
JSSD-6	29.47264	39.90489	18.8	21	22	23	12.2
JSSD-7	29.47703	39.88275	15.6	20.5	29	30	25
JSSD-8	29.48881	39.87583	24.1	21	26.75	26	13.2
JSSD-9	29.48256	39.89553	19.7	20	21.5	22	9
JSSD-10	29.48297	39.90583	24	20.5	35	35	9.6
JSSD-11	29.49414	39.88728	18.2	20.5	18.75	25	11
JSSD-12	29.49772	39.87847	19.6	20.5	20.5	27	9
JSSD-13	29.50558	39.88031	18.2	20	13.5	14	10.2
JSSD-14	29.48881	39.92533	19.7	20.5	26.5	28	10
JSSD-15	29.47997	39.97631	19.7	20	20	36	10
JSSD-16	29.47456	39.99475	19.7	20.5	18	30	10.2
JSSD-17	29.46208	40.01961	19.7	20	19.75	30	10.5
JSSD-18	29.46408	40.0045	19.7	20.5	19	26	9.3
JSSD-19	29.46828	39.98547	19.7	20.5	20	30	20
JSSD-20	29.46311	39.97514	19.7	20.5	20.75	25	9.8
JSSD-21	29.45828	39.99378	19.8	20.5	22	22	11
JSSD-22	29.45289	40.01347	19.8	20	21.5	23	10
JSSD-23	29.442	40.00039	19.7	21	21.5	25	11.7
JSSD-24	29.44906	39.98267	19.7	20.5	22	25	9
JSSD-25	29.44561	39.97286	17.4	20	20	28	9.5
JSSD-26	29.43039	39.99086	19.7	20.5	28.5	30	9.7
JSSD-27	29.42069	40.01319	19	20.5	21.75	29	22.5

The survey area was found to be very transparent (i.e. clean sands) to GPR signals, and exploration depths in excess of 20 meters were achieved in most of the area. The broad area covered with GPR allowed a clear understanding of the sandy plain area structure. Ground truth for the GPR interpretations was obtained by comparing the results with samples representing a total number of twenty-seven core holes. The higher frequencies in the 200 MHz image offer the best vertical resolution with up to 8m depth, and the 100MHz image has intermediate resolution with the greater depth of investigation (nearly 20m for this study).

The MASW shear wave velocity values were found equal to, or slightly different from, the corresponding core hole values. Differences among the core control downhole and the MASW shear wave velocities might be due to averaging out the MASW shear velocities in vertical and lateral extension. Overall both, the core hole values and the MASW shear wave velocities data were found in agreement that validates the results obtained from the MASW method (see Table 2 and 3). On average, MASW estimated that the depth to the bedrock at the existing core holes' locations varies from the core holes' depths to the top of the bedrock by $\sim + 10$ (20 meters). The average difference between depths is found very by both of the methods.

Table 3: Ranking of core control, GPR and MASW

Tool	Core holes	GPR (200 MHz) GPR (100 MHz)	MASW	Seismic refraction
Crew size	3	1	2-3	2-3
Time	2 days	3 hours	3 hours	3 hours
Functionality (acquisition)	4	2	1	3
Accuracy	1	2	1	2
Overall utility	9	2	1	4

Application of geophysical methods is an excellent alternative to the traditional Core hole methods to acquire information by performing a 1-D or 2-D, easy field acquisition, processing and interpenetrations. Each of these methods has been successful, to varying degrees, in replicating the results obtained by the Core holes' measurements. This study was conducted on the silica sand deposits, and the results may not be equally valid at other test sites particularly if the geologic conditions are significantly different. It was not required to access the top of the bedrock due to the expensive drilling operation as the current depth of investigation was sufficient for the study. There were no isolated bedding features observed within the entire sand deposit that confirm as this friable fine sand.

The results of this study (the geophysical site investigation performed using GPR and MASW methods) were validated from the core hole results.

6. Conclusion

The use of GPR was found very effective because of the rapid profiling and initial interpretations with minimal data processing for shallow geophysical investigation (i.e. to estimate thickness of sand depths up to 20m). The GPR depth of penetration is limited compared with the MASW method, but it is more effective to map bedding planes within sand, dry, sandy to seeing the space between layers to better understand depositional environment. A reasonable correlation was observed between the radar and the geological section, especially the results obtained from using the lower frequency antenna (100 MHz shielded GPR), that clearly displays the subsurface layered sands up to 20 meters depth. This made is possible to identify the areas with succession of silica deposits/layers and places that are made up of areas with no noticeable surface layer.

The MASW velocity profile were found in agreement with the core holes' measurements. The evaluation of MASW-estimated bedrock depth values and proximal ground truth (core holes sites) are identified as equal to, or slightly different from, the corresponding core holes' downhole values.

Overall, both the Core holes and the MASW shear wave velocities' data compares favourably, which gives confidence of the MASW method (see Table 2). The author believes also that the differences in the depths are due to the geophysical possibilities, to penetration, or to topographic variation of the subsurface. So, there are areas of low velocity and low density that correspond with the subsurface structure, such as the depth of the silica sand about the top of the bedrock or sandstone.

This study clearly indicates the usefulness of both of the applied geophysical methods in investigating the thickness of silica sand deposits in the vicinity of Dawmat Al Jandal, Al Jawf in Saudi Arabia. The study also helped in reducing the drilling cost remarkably as results of these surveys showed satisfactory correlations between the estimated and actual values.

References

- [1] A. P. Annan, and J. L. Davis, "Design and development of a digital ground penetrating radar system", Pilon, J. (Ed.), Ground Penetrating Radar. Geological Survey Canada, Pap, vol. 90, no. 4, pp. 15-23, 1992.
- [2] L. Pellerin, "Applications of electrical and electromagnetic methods for environmental and geotechnical investigations", Surveys in Geophysics, vol. 23, pp. 101-132, 2002.
- [3] H. Burger, Robert, Sheehan, F. Anne and C.H. Jones, "Introduction to applied geophysics", Exploring the Shallow Subsurface, New York: W.W. Norton, 1st edition (ISBN 0-393-92637-0), p. 624, 2006.
- [4] J. M. Reynolds, "An introduction to applied and environmental geophysics". 2nd edition, John Wiley & Sons Ltd., West Sussex, England, p. 710, 1997.
- [5] O. N. Kovin and N. Anderson, "Use of ground penetrating radar for fracture imaging". Applied Geophysics Conference, pp. 566-573, 2005.
- [6] N. J. Cassidy, "Electrical and magnetic properties of rocks, soils and fluids". In H. Jol (Ed.), Ground Penetrating Radar: Theory and Applications, Solvenia: B. V. Elsevier, pp. 41-72, 2009.
- [7] C. B. Park, R. D. Miller and J. Xia, "Multichannel analysis of surface waves", Geophysics, vol. 64, pp. 800-808, 1999.
- [8] J. Xia, R.D. Miller and C.B. Park, "Estimation of near-surface shear wave velocity by inversion of Rayleigh waves", Geophysics, vol. 64, pp. 691-700, 1999.
- [9] J. Xia, R.D. Miller, C.B. Park and J. Ivanov, "Feasibility of determining Q of near surface materials from Rayleigh waves", [Exp. Abs.]: Soc. Expl. Geophys, pp. 1381-1384, 2001.
- [10] O.N. Kovin, "Ground penetrating radar investigations in upper kama potash mines", (Unpublished Ph.D. Dissertation). Rolla, Missouri, USA: Missouri University of Science and Technology, 2010.
- [11] E.B. Sucre, J.W. Tuttle and T.R. Fox, "The use of ground-penetrating radar to accurately estimate soil depth in rocky forest soils", Forest Science, vol. 57, no. 1, pp. 59-66, 2011.
- [12] B. Choon Park, D.M. Richard, Jianghi Xia and I. Julian, "Multichannel seismic surface-wave methods for geotechnical applications", First International Conference on the Application of Geophysical Methodologies to Transportation Facilities and Infrastructure. St. Louis, USA, pp. 11-15, 2000.
- [13] R.A. Bramkamp, L.F. Ramirez, M. Seineke, and W. H. Reiss, "Geology of the Jawf-Sakakah quadrangle, Kingdom of Saudi Arabia", Geological Survey Saudi Arabian Mission Miscellaneous Geologic Investigations Map I-201A, scale 1:500,000, 1963.

- [14] H.M. Jol and D.G. Smith, "Ground penetrating radar of northern lacustrine deltas", *Canadian Journal of Earth Sciences*, vol. 28, pp. 1939-1947, 1991.
- [15] B. Choon Park, D.M. Richard, Xia Jianghai, R. Nils and U. Peter, "The MASW method - what and where it is", EAGE 65th Conference and Exhibition, Stavanger, 2003.
- [16] B. Choon Park, "MASW horizontal resolution in 2d shear-velocity (vs) mapping", Open-File Report, Lawrence: Kansas Geologic Survey, 2005.
- [17] B. Choon Park, R.D Miller, J. Xia and J. Ivanov, "MASW– An easy seismic method to map shear wave velocity of the ground", Chun Cheon: Korean Society of Engineering Geology, 2004.
- [18] W.R. Emmett, K.W. Beaver and J. A. McCaleb, "Little buffalo basin tensleep heterogeneity – its influence on infilling drilling and secondary recovery", *Journal of Petroleum Technology*, vol. 23, nos. 2, pp. 161-168, 1971.